

Article

Characterization of Surface Topography Features for the Effect of Process Parameters and Their Correlation to Quality Monitoring in Metal Additive Manufacturing

Jinsun Lee ¹, Md Shahjahan Hossain ¹, Mohammad Taheri ², Awse Jameel ³ , Manas Lakshmipathy ³ and Hossein Taheri ^{1,*} 

¹ Laboratory for Advanced Non-Destructive Testing, In-Situ Monitoring and Evaluation (LANDTIE), Department of Manufacturing Engineering, Georgia Southern University, Statesboro, GA 30458, USA; jl08339@georgiasouthern.edu (J.L.); mh31604@georgiasouthern.edu (M.S.H.)

² Department of Mathematics and Statistics, South Dakota State University, Brookings, SD 57007, USA; mohammad.taheri@jacks.sdstate.edu

³ Polytec, Inc., 47909 Halyard Drive, Plymouth, MI 48170, USA; ajameel@polytec.com (A.J.); m.lakshmipathy@polytec.com (M.L.)

* Correspondence: htaheri@georgiasouthern.edu; Tel.: +1-(912)-478-7463

Abstract: Layering deposition methodology in metal additive manufacturing (AM) and the influence of different processing parameters, such as energy source level and deposition speed, which can change the melt pool condition, are known to be the important influencing factors on properties of components fabricated via AM. The effect of melt pool conditions and geometry on properties and quality of fabricated AM components has been widely studied through experimental and simulation techniques. There is a need for better understanding the influence of solidified melt pool topography on characteristics of next deposition layer that can be applied to complex surfaces, especially those with sparse topographical features, such as those that occur in AM deposition layers. Topography of deposited layers in metal additive manufacturing is a significant aspect on the bonding condition between the layers and defect generation mechanism. Characterization of the topography features in AM deposition layers offers a new perspective into investigation of defect generation mechanisms and quality evaluation of AM components. In this work, a feature-based topography study is proposed for the assessment of process parameters' influence on AM deposition layers topography and defect generation mechanism. Titanium alloy (Ti6Al4V) samples deposited on steel substrate, by direct energy deposition (DED) AM technique at different process conditions, were used for the assessment. Topography datasets and analysis of shape and size differences pertaining to the relevant topographic features have been performed. Different AM process parameters were investigated on metallic AM samples manufactured via direct energy deposition (DED) and the potential defect generation mechanism was discussed. The assessment of the topography features was used for correlation study with previously published in-situ monitoring and quality evaluation results, where useful information was obtained through characterization of signature topographic formations and their relation to the in-situ acoustic process monitoring, as the indicators of the manufacturing process behavior and performance.

Keywords: additive manufacturing; direct energy deposition; surface metrology; surface roughness; profile roughness; porosity; crack



Citation: Lee, J.; Hossain, M.S.; Taheri, M.; Jameel, A.; Lakshmipathy, M.; Taheri, H. Characterization of Surface Topography Features for the Effect of Process Parameters and Their Correlation to Quality Monitoring in Metal Additive Manufacturing. *Metrology* **2022**, *2*, 73–83. <https://doi.org/10.3390/metrology2010005>

Academic Editor: Han Haitjema

Received: 13 September 2021

Accepted: 29 January 2022

Published: 7 February 2022

Publisher's Note: MDPI stays neutral with regard to jurisdictional claims in published maps and institutional affiliations.



Copyright: © 2022 by the authors. Licensee MDPI, Basel, Switzerland. This article is an open access article distributed under the terms and conditions of the Creative Commons Attribution (CC BY) license (<https://creativecommons.org/licenses/by/4.0/>).

1. Introduction

The study of surface topography can have different applications in process development, as well as quality assessment. In terms of process development, since the topography of the surface is a function of the process parameters, topography measurements can be utilized to monitor and modify the process parameters, specifically in additive manufacturing,

where the effect of process parameters are significant on the production characteristics. In quality inspection and control, topography information provides fundamental knowledge about the surface finish condition, which is one of the major influencing factors on defect generation, such as crack initiation and propagation and generation of stress concentration locations. Surface topography metrology techniques have been widely used for evaluation of surface and finishing process conditions in additive manufacturing (AM). Investigation of surface characteristics as the signatures of the additive manufacturing process is very useful for AM process development and optimization [1,2]. The recent advancements in high-resolution and high-accuracy 3D geometric models of surface topography can be used for the investigation of the effects of manufacturing process conditions on the quality and surface topography of the parts. These advancements and capabilities also provides the opportunity to acquire high level of details of morphology and topography of deposited AM materials [3]. Specifically, when the surface topography information is used along with the in-situ process monitoring [4,5] and defect generation mechanism [6] in AM, it provides valuable insight into understanding the AM process and quality of the parts. In additive manufacturing technology, feeding materials (usually powders or wires) are deposited on a substrate in a form of layers in a pre-defined sequence. One of the important consequences of this manufacturing approach is that the quality of the final part is a function of the quality of each layer. Additionally, the properties of each deposited layer have significant influence on the characteristics of the next layer. While these characteristics increase the complexity and challenges of quality evaluation for AM parts, it also provides the opportunity for in-situ evaluation and monitoring prior to moving on to the processing of the next layer. Surface topography, which can be quantified, plays an important role in the potential generation of flaws and discontinuity. The morphology and topography of a deposited layer are the result of the manufacturing process and contain important information about the deposition process and future quality of the parts [7–9]. Processing conditions in metal additive manufacturing not only affect the macro-mechanical properties, but also influence the morphology of the layer. Raw material properties [10] and manufacturing process conditions, such as input energy (laser power), feed rate of raw materials, hatch distance [11], layer thickness, and scanning speed [12], have been reported to play important roles in surface morphology and topography of AM parts. In addition to the manufacturing processing conditions, properties of the feedstock, rheology and the temperature of the melting pool have been shown to cause variation of surface tension and formation of the surface profile [13]. Melt pool conditions, such as geometry (dimension), stability and behavior, determine both surface roughness and flaws (porosity or cracks) of AM-fabricated parts [14]; hence, it is necessary to understand the relation of these two parameters. Newton et al. (2018) studied the evolving surface topographies in finishing operations for additive manufacturing. In Newton's approach, a feature-based technique was used to identify the topography formations and track their changes after finishing operations [15]. Up to a 30% decrease in value of roughness was reported by Khorasani et al. [13] when increasing laser power in laser powder bed fusion (LPBF) manufacturing of Ti-6Al-4V samples. Several different surface topography features can be used to evaluate the surface characteristics and study the properties of the AM parts. A lower S_q (root mean square value of ordinate values within the definition area) and S_{dq} (general measurement of the slopes that comprise the surface and may be used to differentiate surfaces with similar average roughness) values were observed for samples produced with high power and similar scan speed by Thanki et al. (2020) [16]. Nagalingam et al. [17] have discussed the challenges in surface properties measurement for AM components due to various asperities and random roughness distributions. They have concluded that traditional measurements based on available standards, such as ISO 4287, 4288, and 25178, need some level of adjustment; they proposed a framework for such modifications. Nagalingam's findings confirm the current paper's approach in application of more detailed measurement and, using Gaussian filters to enhance isolating the relevant features in surface topography, measurements that can be used for AM process

development and quality inspection [17]. However, there are several research studies on surface characterization of AM parts and influence of processing parameters on surface topography but understanding the relation of these parameters to the quality of the parts and defect generation mechanism is still a big gap in additive manufacturing technologies. The aim of this study is to evaluate the surface topography features generated at different additive manufacturing process conditions and to understand the relation between the manufacturing process conditions, topography features, defect generation mechanism, and possibility of the correlation to in-situ process monitoring results obtained through acoustic signatures of the manufacturing process in a former study.

2. Methodology

2.1. Samples

Titanium alloy (Ti-6Al-4V) samples were fabricated by the direct energy deposition (DED) technique on a tool steel baseplate. In DED additive manufacturing, the continuously delivered powder or wire raw material is melted by a laser as a focused heat source to fabricate the final geometry of the parts [18]. Titanium alloys are widely used in aerospace and bio-medical applications because of their outstanding characteristics, such as high strength, low density, and superior corrosion resistance. In this study, the samples were built at different process conditions, to include process-related effects due to process parameters in the investigation. Different process condition that have been considered include normal (optimum), low power density, and low powder feeding rate, as described in Table 1 [4].

Table 1. Different direct energy deposition (DED) process conditions.

Process Condition Number	Description	Abbreviation
Condition 1	Optimum (Normal)	C1
Condition 2	Low Laser Power	C2
Condition 3	Low Powder Feed	C3

Different depositions of the titanium alloy were positioned on random locations on the steel base plate. Five samples at each different process conditions (Table 1) were made. All samples that were 25 mm × 5 mm and had only one (1) deposited layer were cut using electrical discharge machining (EDM) for further processing and microscopy testing.

2.2. Measurement Setup

The samples were measured on a Polytec Micro. View optical profiler (Polytec, Boston, MA, USA) using 10× objectives. The fundamental measurement principal is governed by the technique universally called as coherence scanning interferometry using a broadband white light source. The white light interferometer is an optical measuring system that takes advantage of the short-coherence property of white light. Using a beam splitter, the light emitted by an LED is divided into a measurement path and a reference path. Interference only occurs when the optical path length difference between the measurement and the reference arms is less than half the coherence length. While the reference path is terminated by a mirror, the light from the measuring path is reflected by the target surface. An image sensor records the super-imposed reflections of the measurement and reference paths. The Mirau objective, used for magnification between 10× and 100×, has an integrated micro-mirror that is located at a small distance from a beam splitter. The reference path in a Michelson objective (typically magnifications up to 5×), on the other hand, is in a separate arm of the lens. The above interferometer designs are shown in Figure 1.

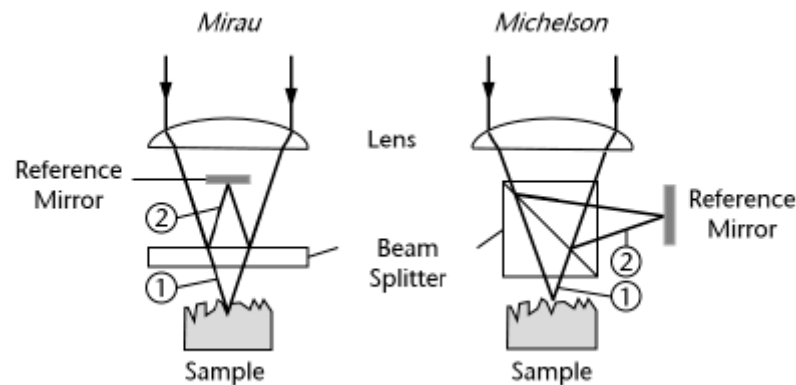


Figure 1. Setup of a white light interferometer for microscopic surface measurements.

During a measurement, the length of the measuring path was continuously changed (by moving the objective via a piezo scanner or motorized Z stage), allowing it to span the entire height of the tested surface. As interference occurred, the intensity modulation of the light (the correlogram) was detected. Each pixel's correlogram was continuously stored for the entirety of the scan length, see Figure 2.

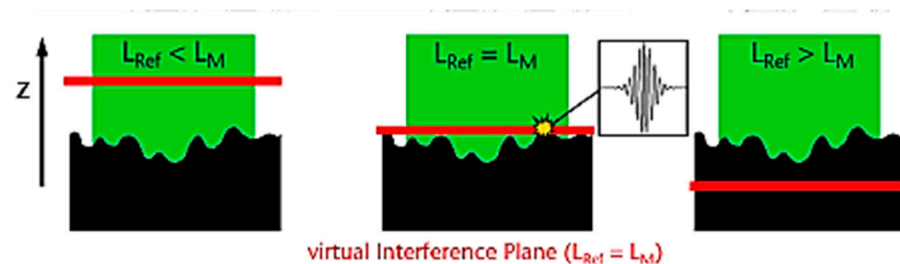


Figure 2. Time sequence of a scanning measurement: If the correlogram has been scanned for all pixels, the measurement can be terminated.

The scanning sequence, therefore, stored the history of all the pixels' change in intensity. Taking into account the position of the scanner and the maximum contrast of the pixel, the software was then able to lay out all the points in relation to each other. The z-value of the point on the surface that was depicted on this pixel corresponded to the z-value of the positioning stage when the modulation of the correlogram was at a maximum. Thereafter, the TMS software could process this raw information into images and topography results. Measurements have been conducted over the $200 \mu\text{m} \times 200 \mu\text{m}$ area of all samples at different locations with $10\times$ magnification.

3. Surface Topography Feature Characterization

3.1. 3D Topography Features

The 3D topography of the samples shows the difference of the feature at each process condition, as shown in Figure 3. In the C1 process condition (Figure 3a), more uniformly-distributed surface topography features were observed. In addition, the change in the height at the location of these feature was slightly shifting from the surrounding area to the spatters. However, in the C2 process condition (Figure 3b), a higher surface roughness with a larger number of spatters was observed. In this condition, the spatters had more abrupt changes in their heights. This could be explained as the influence of some un-melted or partially melted powder particles on each subsequent layer in the C2 process condition. The abrupt changes in the topography of the layer surface could be the major cause of lack-of-fusion (LOF) porosity in this situation. Finally, in the C3 process condition (Figure 3c), in addition to the separated random distribution of the spatters, a clear sign of cracking could

be seen in the surface topography, which could be due to lower concentration of material and higher thermal gradients.

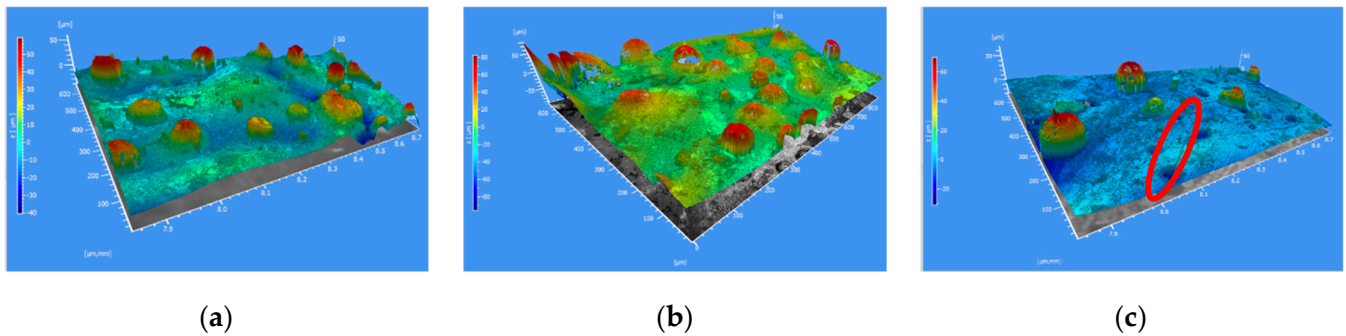


Figure 3. 3D topography of the samples (a) Normal Condition, (b) Low power, (c) Low powder.

3.2. Surface Area Features Measurement

Surface topography parameters, including arithmetic average areal roughness values (S_a) and arithmetic average linear roughness values (R_a), have been measured for each sample. The S_a values have been measured over the $200\ \mu\text{m} \times 200\ \mu\text{m}$ area of all samples at different locations with $10\times$ magnification. Comparison of average and standard deviation for the S_a of the samples at different manufacturing processing conditions is presented in Table 2.

Table 2. Comparison of arithmetic average roughness values (S_a) of the AM samples at different manufacturing processing condition.

Sample Number	C11, C12	C21, C22	C31, C32
Manufacturing Processing Condition	Normal	Low Power	Low Powder
S_a [μm] (average value over the area)	5.1	10.3	2.3
Standard deviation [μm]	2	2.9	0.7

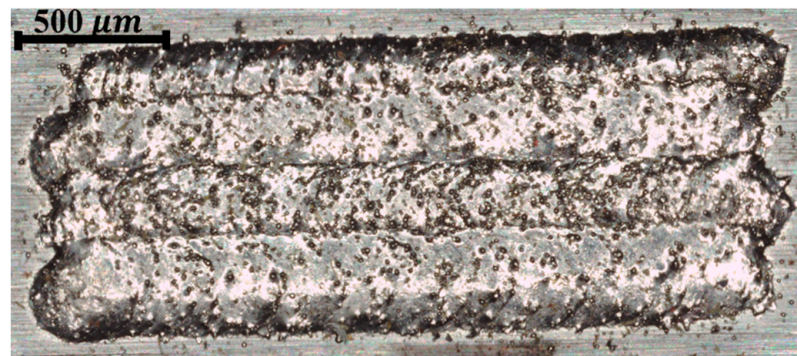
The higher S_a values in low power manufacturing process condition could be interpreted as the lack of input energy for melting the metal powders during the deposition, which caused a portion of the powders to be partially melted or just sintered to the surrounding materials and created localized rough surfaces in the deposited layers. At low power condition, the energy density and melting pool temperature decreased according to Equations (1) and (2) [19,20], where E_d is the energy density, η is the absorption coefficient, L_p is laser power, S_s is scan speed, B_A is beam area, T_0 is the reference value for temperature, T_s is solidus temperature, C_{P_s} is the specific heat capacity in solid state, ΔH_m is the enthalpy phase change for solid to liquid, T_l is liquid temperature, T_{mp} is Titanium melting point temperature and C_{P_m} is the specific heat capacity in liquid state.

$$E_d = \frac{\eta L_p}{S_s B_A} \tag{1}$$

$$E_d = \int_{T_0}^{T_s} C_{P_s} dT + \Delta H_m + \int_{T_l}^{T_{mp}} C_{P_m} dT \tag{2}$$

Lower melt pool temperature, because of the low power, increased the surface tension, which, in turn, leads to an increased Rayleigh instability [21,22]. On the other hand, the lower S_a values in the low powder condition could be due to a lower ratio of the deposited material to the input energy, which caused all powders to completely melt and merge together. In addition, a lower volume of material (powders) in some area of

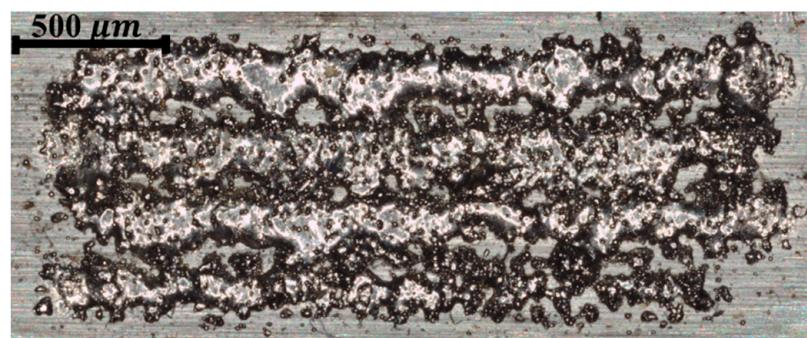
measurement also affected the lower S_a value measurement. The optical microscopy images taken from the samples at different process conditions by optical microscope (OLYMPUS BX53M, Figure 4) and by digital microscope (Keyence VHX 7000, Figure 5) could be used to enhance this understanding. As can be seen from the optical images, there was a significant difference in the surface texture for the different process conditions. As discussed earlier from the surface topography measurement results, a consistent deposition and texture could be seen in the normal process condition, while a thin deposition and fully meted area appeared in the low powder condition and a discontinued rougher texture happens in the low power process condition.



(a)



(b)



(c)

Figure 4. Optical images of the surface textures at different manufacturing process conditions; (a) normal, (b) low powder, and (c) low power.

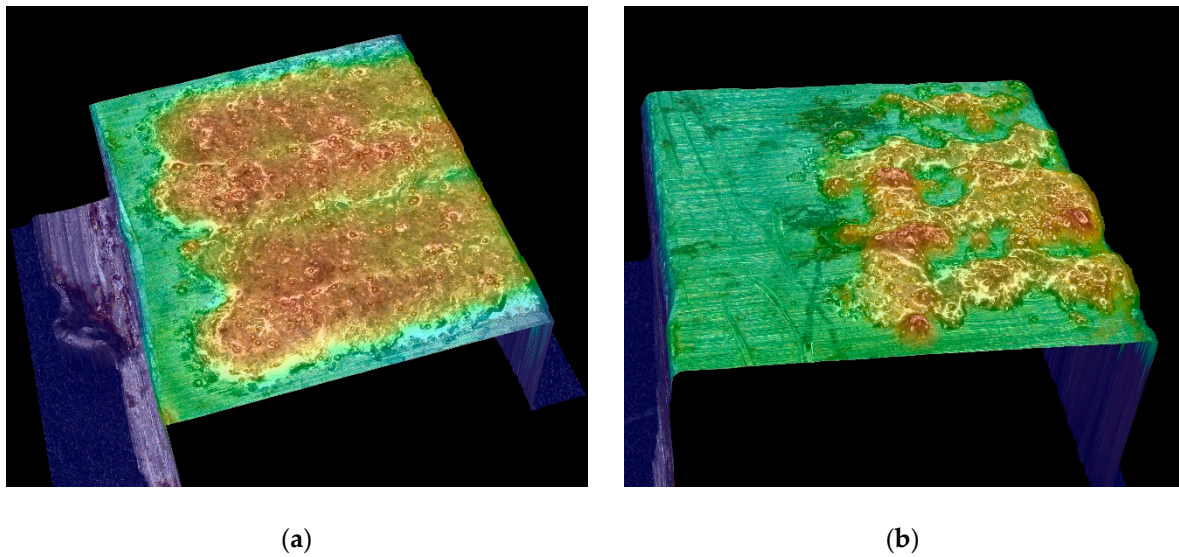


Figure 5. Optical 3D images of the surface textures on a $200\ \mu\text{m} \times 200\ \mu\text{m}$ region of the sample; (a) Normal, (b) Low power process conditions.

4. Quality Assessment Based on Surface Features

It has been shown by several works that the melt pool characteristics and, consequently, the surface topography of each deposition layer, significantly influence the generation of defects such as porosity and keyholes in AM components [23]. From the topography of the specimens at different process conditions (Table 1), the melt pool condition and defect generation indicators could be observed, as shown in Figure 6. In the C1 process condition, a more uniform distribution of the topography features could be seen (Figure 6a). In the C2 condition, a larger density and distribution of porosities at different sizes were visible in the topography, which were due to un-melted regions (Figure 6b). For the C3 condition, the higher concentration of energy caused more uniform melting in the melt pool, which generated lower spikes in the topography in the surface; however, it could also cause the generation of local cracking due to the larger thermal gradient, as can be seen in (Figure 6c).

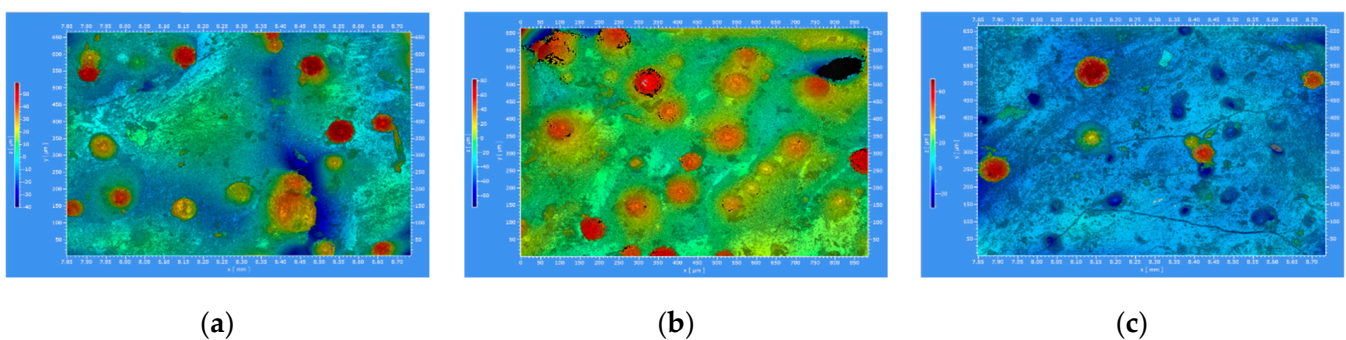


Figure 6. Quality assessment based on surface features at different process conditions. (a) Normal Condition, (b) Low power, (c) Low powder.

The Ra values were also measured for each sample within the same targeted area as described above. The localized peaks that are part of the Ra values in low-power condition (C2) have been identified using a line profile as shown in Figure 7 and measured to be in the range of $40\text{--}50\ \mu\text{m}$, which is comparable to the layer thickness of the deposition process. Inhomogeneity of the surface generated due to these localized spikes in the level of layer thickness is another explanation for the LOF defect generation in this condition.

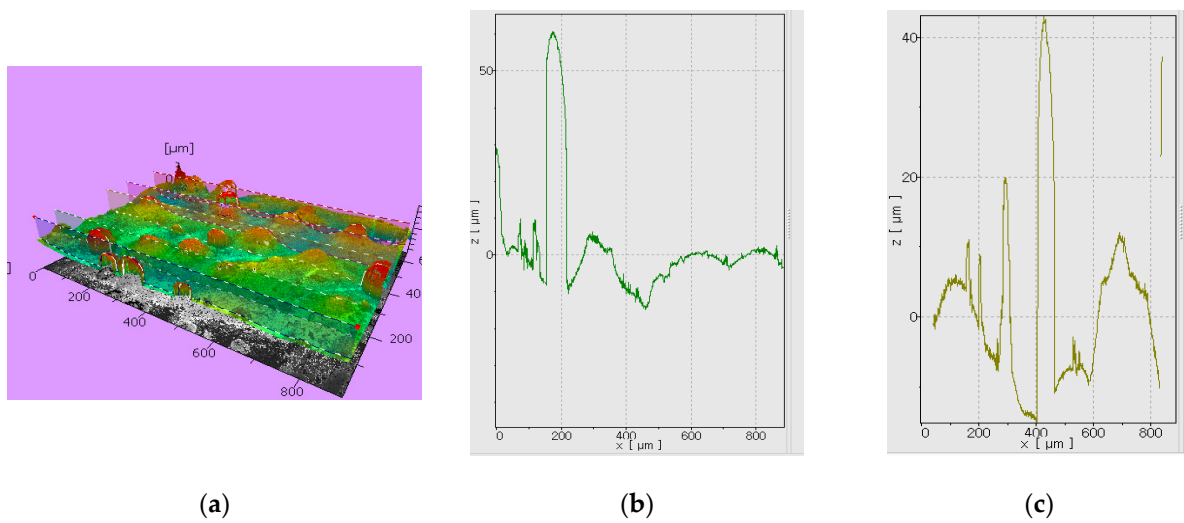


Figure 7. Surface topography measurement of Ra value for AM sample in low-power (C2) processing condition; (a) 3D topography, (b,c) local line profile measurements.

Further processing of the surface topography measurements, such as averaging for every sample point in elliptical or rectangular surroundings, or application of filtering, such as S-filters, will enhance the assessment of the topography measurements for the purpose of quality assessment based on surface features. In the Gaussian low-pass filter application, a 5 μm S-nesting index was used to separate roughness and waviness according to the recommendations in ISO 25178-3. Figure 8 shows the results of applying S-filter to the measurements at different manufacturing process conditions. The filtering process significantly improved the identification of the quality indicators on each sample. For the C2 processing condition, the localized porosities clearly appeared in the measurement results, showing both larger lack-of-fusion (LOF) porosities as well as localized gas porosities, which were mostly concentrated around the spikes of the topography. The cracking that happened at the C3 process condition could be efficiently seen in the filtered measurement images, which show the propagation and geometry of the cracks.

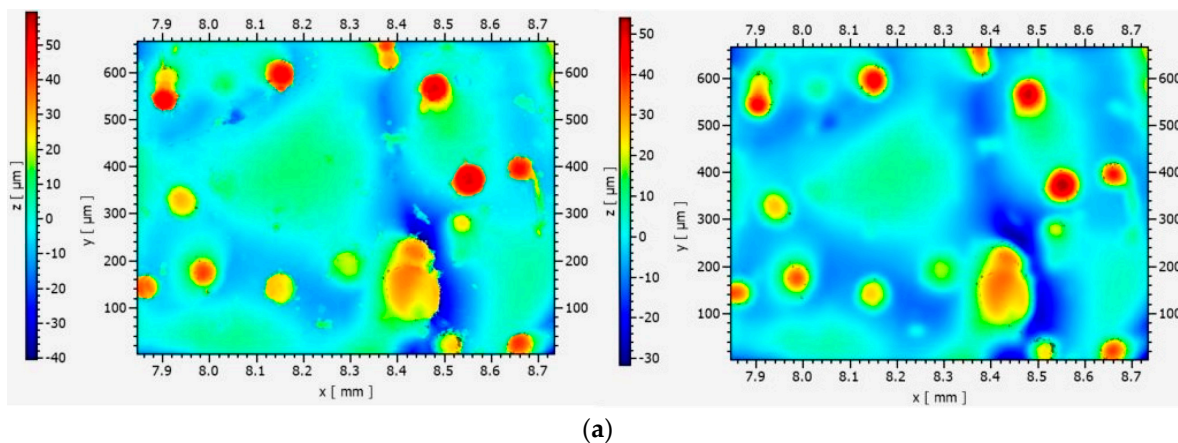


Figure 8. Cont.

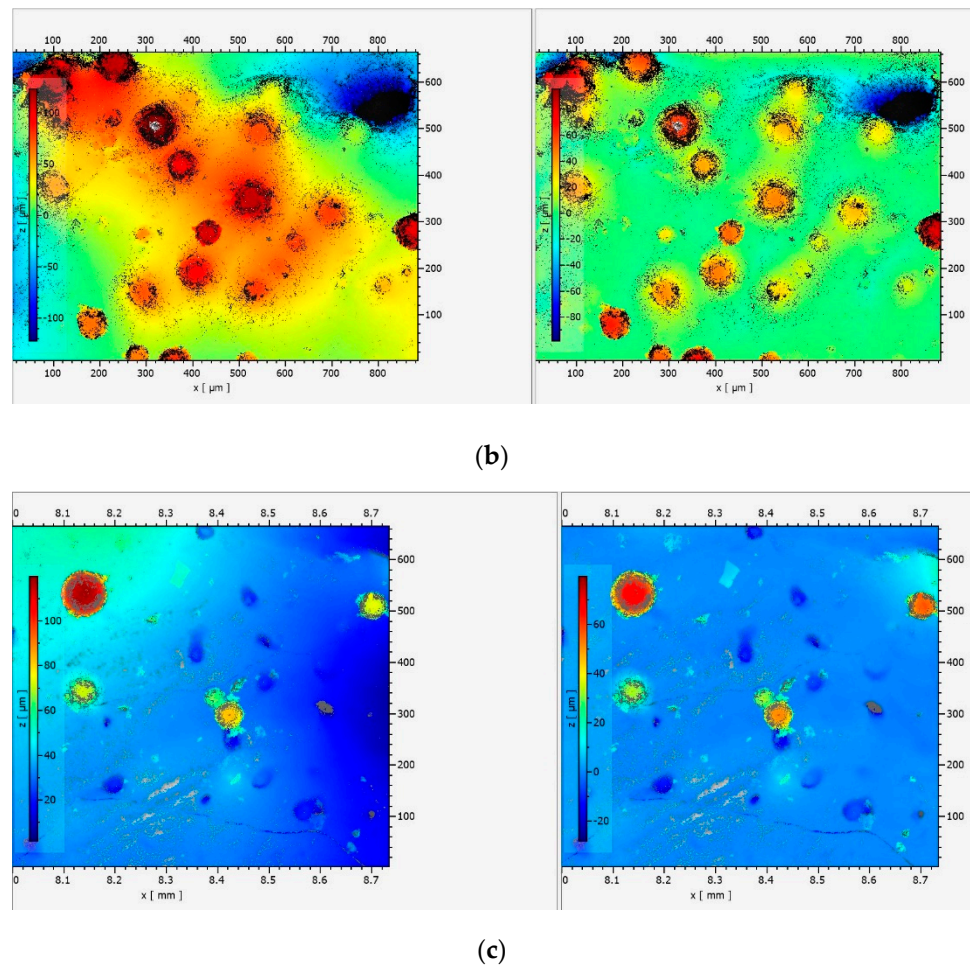


Figure 8. Surface topography of AM samples different processing conditions before and after applying S-filter; (a) C1 process condition; Left: Before filtering, Right: After filtering (y -axis [μm]), (b) C2 process condition; Left: Before filtering, Right: After filtering (y -axis [μm]), (c) C3 process condition; Left: Before filtering, Right: After filtering (y -axis [μm]).

5. Manufacturing Process Monitoring and Quality Control

One of the main goals of layer-wise quality evaluation and understanding of the effect of process conditions on the defect generation and properties of each layer, is to correlate this information to the in-situ process monitoring methods in additive manufacturing technology. Currently, there are a variety of in-situ monitoring processes for additive manufacturing processes to identify any deviation from the optimum processing condition. These in-situ monitoring techniques include thermography, optical imaging and image processing, and acoustic techniques that have been comprehensively discussed in several review papers [5,24]. Following the identification of changes in process conditions, it is necessary to understand the influence of such deviations on the mechanical properties and potential defect generation on the parts. In a previous publication [4], it was shown that the frequency features recorded from the acoustic signatures during the manufacturing of the same samples used in this study could be used to efficiently classify different additive manufacturing process conditions [4]. Since the different manufacturing processing conditions have been identified using acoustic signatures for in-situ monitoring, the next step is to identify the related change in properties of the part due to generation of potential defects and flaws caused by the changes in processing conditions. As described above, the quality assessment of the AM samples based on surface features provides a comprehensive understating of the deposition layer characteristics and defect generation mechanism due

to the layer's topography. Combined with the advancements in in-situ process monitoring, the results of this quality assessment can be used as a valuable inform.

6. Conclusions

Process parameters in metal additive manufacturing, such as level of input energy and rate of feeding raw materials, have shown significant influence on the final quality of the produced parts. Variations in manufacturing processing parameters can be identified by in-situ process monitoring techniques, such as classifying the acoustic signatures recorded during the manufacturing process, and can be correlated to the quality and surface finish of the produced parts. These variations in process parameters cause a change in melt-pool geometry and conditions as well as generation of defects and flaws in the parts. Consequently, changes in processing parameters will critically affect surface topography of each deposited layer and the finished part. Study of surface topography features in this work provided useful insight for the type and conditions of potential flaws that can be generated due to changes in processing conditions, which can be used for correlating to in-situ process monitoring and quality assessment of the additively manufactured parts. Studying the surface characteristics of the deposited metal additive manufacturing at different process conditions showed that, while a more uniform distribution of surface features could be observed in the normal (optimum) manufacturing processing condition, there were abrupt changes in surface characteristics when the manufacturing process deviated from the normal condition, such that one could observe defect generation indications on surface topography.

Author Contributions: Conceptualization, H.T. and M.T.; methodology, M.L. and A.J.; software, M.L. and A.J.; validation, J.L. and M.S.H.; formal analysis, M.L. and A.J.; investigation, M.L., A.J. and J.L.; resources, H.T., M.L. and A.J.; data curation, M.L., J.L. and A.J.; writing—original draft preparation, M.T.; writing—review and editing, H.T.; visualization, M.T.; supervision, H.T.; project administration, H.T. All authors have read and agreed to the published version of the manuscript.

Funding: This research received no external funding.

Institutional Review Board Statement: Not applicable.

Informed Consent Statement: Not applicable.

Data Availability Statement: Not applicable.

Acknowledgments: Authors would like to acknowledge the collaboration with Center for Non-Destructive Evaluation (CNDE) at Iowa State University and machine shop at Department of Manufacturing Engineering at Georgia Southern University (Andrew Michaud) for sample preparation.

Conflicts of Interest: The authors declare no conflict of interest.

References

1. Thomas, T.R. Roughness and function. *Surf. Topogr. Metrol. Prop.* **2013**, *2*, 14001. [[CrossRef](#)]
2. Benardos, P.G.; Vosniakos, G.-C. Predicting surface roughness in machining: A review. *Int. J. Mach. Tools Manuf.* **2003**, *43*, 833–844. [[CrossRef](#)]
3. Senin, N.; Thompson, A.; Leach, R. Feature-based characterisation of signature topography in laser powder bed fusion of metals. *Meas. Sci. Technol.* **2018**, *29*, 045009. [[CrossRef](#)]
4. Taheri, H.; Koester, L.W.; Bigelow, T.A.; Faierson, E.J.; Bond, L.J. In Situ Additive Manufacturing Process Monitoring with an Acoustic Technique: Clustering Performance Evaluation Using K-Means Algorithm. *J. Manuf. Sci. Eng.* **2019**, *141*, 41010–41011. [[CrossRef](#)]
5. Hossain, M.S.; Taheri, H. In Situ Process Monitoring for Additive Manufacturing Through Acoustic Techniques. *J. Mater. Eng. Perform.* **2020**, *29*, 6249–6262. [[CrossRef](#)]
6. Taheri, H.; Shoaib, M.R.B.M.; Koester, L.W.; Bigelow, T.A.; Collins, P.C.; Bond, L.J. Powder-based additive manufacturing—A review of types of defects, generation mechanisms, detection, property evaluation and metrology. *Int. J. Addit. Subtract. Mater. Manuf.* **2017**, *1*, 172. [[CrossRef](#)]
7. Sames, W.J.; List, F.A.; Pannala, S.; Dehoff, R.R.; Babu, S.S. The metallurgy and processing science of metal additive manufacturing. *Int. Mater. Rev.* **2016**, *6608*, 1–46. [[CrossRef](#)]
8. Leach, R. Metrology for Additive Manufacturing. *Meas. Control* **2016**, *49*, 132–135. [[CrossRef](#)]

9. Townsend, A.; Senin, N.; Blunt, L.; Leach, R.K.; Taylor, J.S. Surface texture metrology for metal additive manufacturing: A review. *Precis. Eng.* **2016**, *46*, 34–47. [[CrossRef](#)]
10. Chen, Z.; Wu, X.; Tomus, D.; Davies, C.H.J. Surface roughness of Selective Laser Melted Ti-6Al-4V alloy components. *Addit. Manuf.* **2018**, *21*, 91–103. [[CrossRef](#)]
11. Sanaei, N.; Fatemi, A.; Phan, N. Defect characteristics and analysis of their variability in metal L-PBF additive manufacturing. *Mater. Des.* **2019**, *182*, 108091. [[CrossRef](#)]
12. Yadroitsev, I.; Smurov, I. Surface morphology in selective laser melting of metal powders. *Phys. Procedia* **2011**, *12 Pt 1*, 264–270. [[CrossRef](#)]
13. Khorasani, M.; Ghasemi, A.; Awan, U.S.; Hadavi, E.; Leary, M.; Brandt, M.; Littlefair, G.; O’Neil, W.; Gibson, I. A study on surface morphology and tension in laser powder bed fusion of Ti-6Al-4V. *Int. J. Adv. Manuf. Technol.* **2020**, *111*, 2891–2909. [[CrossRef](#)]
14. Delfs, P.; Tows, M.; Schmid, H.J. Optimized build orientation of additive manufactured parts for improved surface quality and build time. *Addit. Manuf.* **2016**, *12*, 314–320. [[CrossRef](#)]
15. Newton, L.; Senin, N.; Smith, B.; Leach, R. Feature-based characterisation of evolving surface topographies in finishing operations for additive manufacturing. In Proceedings of the 18th International Conference and Exhibition (euspan), Venice, Italy, 4–8 June 2018; pp. 489–490.
16. Thanki, A.; Witvrouw, A.; Haitjema, H. Effect of process parameters on the surface topography formation in precision additive metal manufacturing. In Proceedings of the Euspen 20th Interfantional Conference & Exhibition, Northampton, UK, 8–12 June 2020. [[CrossRef](#)]
17. Nagalingam, A.P.; Vohra, M.S.; Kapur, P.; Yeo, S.H. Effect of cut-off, evaluation length, and measurement area in profile and areal surface texture characterization of as-built metal additive manufactured components. *Appl. Sci.* **2021**, *11*, 5089. [[CrossRef](#)]
18. Saboori, A.; Gallo, D.; Biamino, S.; Fino, P.; Lombardi, M. An overview of additive manufacturing of titanium components by directed energy deposition: Microstructure and mechanical properties. *Appl. Sci.* **2017**, *7*, 883. [[CrossRef](#)]
19. Gibson, I.; Rosen, D.; Stucker, B. *Additive Manufacturing Technologies*, 3rd ed.; Springer: New York, NY, USA; Heidelberg, Germany; Dordrecht, The Netherlands; London, UK, 2020.
20. Holman, J.P. *Heat Transfer*; McGraw-Hill: New York, NY, USA, 1986.
21. Li, R.; Liu, J.; Shi, Y.; Wang, L.; Jiang, W. Balling behavior of stainless steel and nickel powder during selective laser melting process. *Int. J. Adv. Manuf. Technol.* **2012**, *59*, 1025–1035. [[CrossRef](#)]
22. Mahamood, R.M.; Akinlabi, E.T. Scanning speed and powder flow rate influence on the properties of laser metal deposition of titanium alloy. *Int. J. Adv. Manuf. Technol.* **2017**, *91*, 2419–2426. [[CrossRef](#)]
23. Kumar, P.; Farah, J.; Akram, J.; Teng, C.; Ginn, J.; Misra, M. Influence of laser processing parameters on porosity in Inconel 718 during additive manufacturing. *Int. J. Adv. Manuf. Technol.* **2019**, *103*, 1497–1507. [[CrossRef](#)]
24. Everton, S.K.; Hirsch, M.; Stravroulakis, P.; Leach, R.K.; Clare, A.T. Review of in-situ process monitoring and in-situ metrology for metal additive manufacturing. *Mater. Des.* **2016**, *95*, 431–445. [[CrossRef](#)]